Research Article
Five-fold Symmetric Photonic Quasi-crystal Fiber with High Negative Dispersion

Sivacoumar Rajalingam and Z.C. Alex
School of Electronics Engineering, VIT University, Vellore, Tamil Nadu, India

Abstract: Dispersion causes optical pulses broadening and must be compensated for in long-distance high-speed optical data transmission systems. We investigate optical properties of micro structured fiber with 5-fold symmetric quasicrystal lattice of air-holes in a silica matrix for the first time. Dual-Concentric core Photonic Quasicrystal Fiber (DC-PQF) lattices with varying hole diameters were investigated and curves for the effective index, dispersion parameter and confinement losses were calculated by finite element method. For dispersion compensation purpose, we have proposed a novel 5-fold PQF with a high negative dispersion values ≈ 16,000 ps/(nm-km) could be reached for the wavelength around 1310 nm.

INTRODUCTION

The control of Chromatic Dispersion (CD) is crucial for optical networks and nonlinear applications. Single-mode fibers, used in high-speed optical networks, are subject to chromatic dispersion that causes pulse broadening depending on wavelength and Polarization Mode Dispersion (PMD) depending on polarization states (Zografopoulos *et al.*, 2011). The signal degrades and limits the distance a digital signal can travel before needing regeneration or compensation. An optical network, operated at 1550 nm using a standard ITU G.652 fiber having chromatic dispersion of 17 ps/(nm-km) curtails to a maximum transmission distance of 60 km. Penalties incurred by chromatic dispersion can be minimized using negative Dispersion Compensating Fibers (DCF). The commercial dispersion compensation fibers usually have chromatic dispersion of -100 to -300 ps/(nm-km) (Birks *et al.*, 1999; Chin-Ping *et al.*, 2008). To ensure higher negative dispersion, doped high-index core and small effective mode area are widespread in DCF designs, eventually culminating higher scattering loss and nonlinear effects. Photonic Crystal Fibers (PCF) can speculate very high negative dispersion due to high index difference between core and conformable cladding. PCF structures with high index inner core and a defected ring of reduced holes in the cladding comparable to dual core geometries have accomplished dispersion as high as -2200 ps/(nm-km) (Gerome *et al.*, 2004; Abdur Razzak *et al.*, 2010). Doping of higher percentage of GeO$_2$ leads to interference of higher order modes inducing modal noise. Quasi-periodic structures are self-similar lattice generated by inflation-deflation procedure of matching rules with long-range order with no periodicity. It has been evident that quasi-periodic structures can give rise to unusual phenomena and desired properties like large cut off ratio for endlessly single mode operation, ultra-flat dispersion (Jianfei *et al.*, 2013), etc., not been observed in periodic structures (Zoorob *et al.*, 2000; Kim *et al.*, 2007; Kim and Kee, 2009; Fleming, 1984).

To realize dispersion compensation, in this research paper, we propose a 5-fold Dual-Concentric-core Photonic Quasi crystal Fiber (DC-PQF), designed to achieve high negative dispersion control over a wide range of telecom wavelength with symmetrical mode confinement and improved effective mode area.

DESIGN METHODOLOGY

We have illustrated the cross section of 5-fold DC-PQF in Fig. 1. The PQF structure is formed by two types of rhombic tiles, thin tile with angles of 36° and 144° and thick tile with angles of 72° and 108°. The resulting connected space-filling packing of unit cells is called Penrose lattice. The inner core and the surrounding air holes are constructed on the base of 2-dimenstional Penrose lattice. The inner core of PQF, with a diameter of 1.8 μm (d$_{core}$) is doped with very low concentration of Germanium contributing an index difference of 1.92%. The outer defected core is a pure fused silica core formed by eliminating the second ring of 15 air holes. In our analysis the refractive index of fused silica as a function λ is calculated using sellmeier equation (Fleming, 1984):

Corresponding Author: Sivacoumar Rajalingam, School of Electronics Engineering, VIT University, Vellore, Tamil Nadu, India
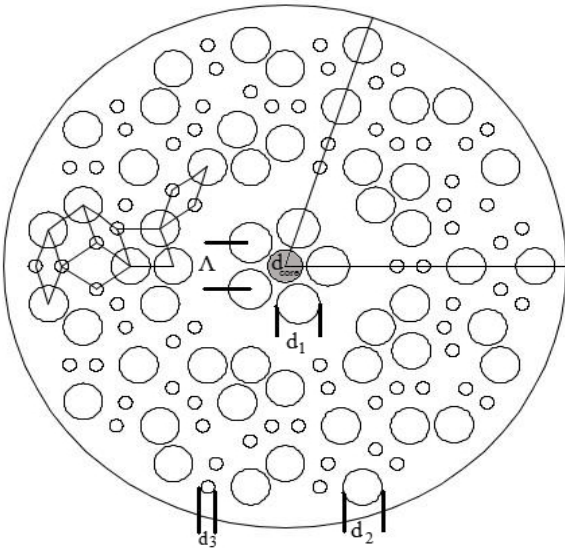
Fig. 1: Cross section of proposed 5-fold symmetric DC-PQF with d_1 = 2.2 μm, d_2 = 1.8 μm, d_3 = 0.7 μm and the inner core diameter d_{core} = 1.8 μm doped with germanium

$$n^2(\lambda) = 1 + \sum_{i=1}^{3} \frac{A_i \lambda^2}{\lambda^2 - B_i^2} \tag{1}$$

where, λ is the wavelength of incident light and n is the refractive index of silica. The coefficient of Sellmeier "A_i" is the oscillator strengths of transitions and "B_i" is the squares of the respective transition energies (as photon wavelengths). We set A_1 = 0.96166300, A_2 = 0.407942600, A_3 = 0.897479400, B_1 = 0.00467914826, B_2 = 0.0135120631 and B_3 = 97.9340025 for fused silica in our calculations, respectively.

Inner cladding is formed between the two cores with hole diameter of 2.2 μm (d_1). We have maintained 2.2 μm between core to first cladding ring and there by the lattice constant or pitch (Λ) was computed to be 2.609 μm, since lattice was constructed as 5 fold symmetry. In this design, we have designated outer cladding air holes with two different diameters 1.8 μm (d_2) and 0.7 μm (d_3). The air hole in the cladding depresses the average index of the cladding region and confines light within the central core (Aliramezani and Mohammad Nejad, 2010). The highest negative dispersion can be tailored with suitable design of these three parameters d_1, d_2 and d_3 and with careful doping concentration of core diameter the phase matching peak wavelength can be shifted to a commodious value. The air filling ratio of the lattice with 0.84 ($d_1/Λ$), 0.69 ($d_2/Λ$) and 0.27 ($d_3/Λ$) for inner and the outer core is maximized by the quasilattice distribution.

We employed Finite Element Method (FEM) with anisotropic Perfectly Matched Layers (PML) to assess the effective index of the core mode in PCF. Many optical properties such as Dispersion parameter (D), group velocity dispersion ($β_2$), confinement loss and birefringence and so on can be numerically investigated. The field distribution is observed along with the real and imaginary part of n_{eff}. By including PML, the resultant fully vectorial wave equation is derived from the Maxwell's equations as:

$$\nabla \times \left([\mu]_{PML}^{-1} \nabla \times E \right) - k_0^2 [\varepsilon]_{PML} E = 0 \tag{2}$$

where, k_0 is the free space wave number and E is the electric field vector. The parameters $[\mu]_{PML}$ and $[\varepsilon]_{PML}$ are the permittivity and permeability tensors of the PML regions, respectively.
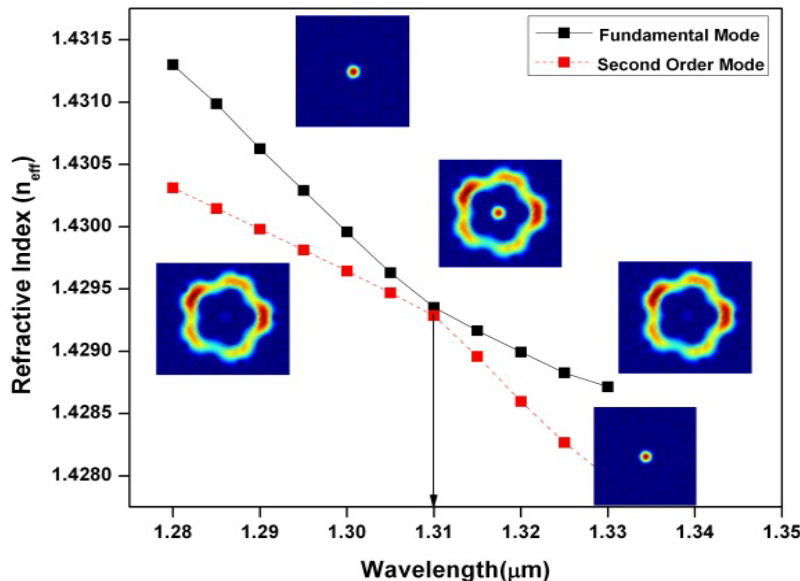

Fig. 2: Variation of effective refractive index with wavelength for DC-PQF, a solid curve corresponds to a fiber with fundamental core and dashed cure represents outer mode. Inset figure shows the changeover of modes
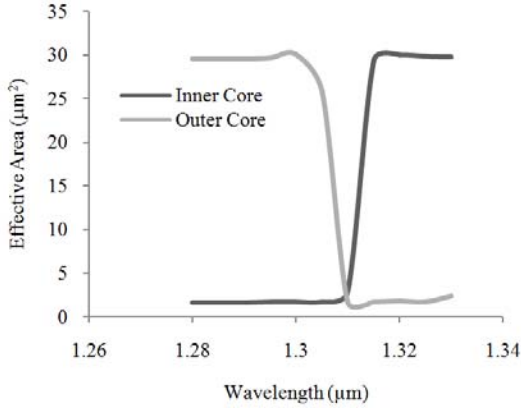
Fig. 3: The effective area of the inner core mode and the outer core mode, showing drastic change during the phase matching conditions

Figure 2 shows the variation of effective refractive index (n_{eff}) of fundamental inner core mode and second order mode of outer core with reference to wavelength. It is found that the effective refractive index of the inner core mode and outer core mode matches with each other at phase matching wavelength (λ_p). Before the phase matching wavelength ($\lambda < \lambda_p$), the field distribution of the inner core mode is confined within the central core and is a Gaussian shape. After the phase matching wavelength ($\lambda > \lambda_p$), the fundamental mode field distribution is in the outer core region.

The splicing loss is attributed to the mismatch between the two modes of PCF-SMF splices (Kliros *et al.*, 2007). The splicing loss α, caused by mode conversion could be calculated by the calculating the overlap integral:

$$\alpha(\text{db}) = -10\log\left[\frac{\int\left(E_{PCF}E_{SMF}dA\right)}{\sqrt{\int\left(E_{PCF}E_{PCF}dA\right)\int\left(E_{SMF}E_{SMF}dA\right)}}\right]^2 \quad (3)$$

where, E_{PCF} and E_{SMF} are the transverse electric-field distributions of the two modes in PCF and SMF, respectively. In order to take the effective mode area into consideration, it is evaluated, according to:

$$A_{eff} = \frac{\left(\iint_s |E_t|^2\,dxdy\right)^2}{\left(\iint_s |E_t|^4\,dxdy\right)} \quad (4)$$

where, E_t is transverse electric field intensity of core mode and the integrals are over the entire cross section of the dual-core PCF.

We can observe in the Fig. 2 fundamental mode field distribution confined within the core and the second order mode trapped within the outer core twitch

towards each other as the operating wavelength changes. It is evident that at a point of inflexion (λ_p = 1.31 μm) slope of effective refractive index changes due to coupling of mode energy from inner to outer and contrariwise. At phase matching condition the effective mode field area of 3.2 μm^2 inflates to a very large value of 80.1 μm^2. The confinement loss is deduced from the value of n_{eff} as:

$$\text{Confinement Loss} = 8.686\,\text{Im}\,[k_0\,n_{eff}] \quad (5)$$

in dB/m, where Im stands for the imaginary part of effective refractive index. The confinement loss for the inner core mode at 1.28 μm is 2.0×10^{-6} dB/m increases to 1.27×10^{-3} dB/m at phase matching wavelength. The splicing loss with standard SMF28 is minimized to a large extent as the effective mode area is in agreement with single mode fiber (White *et al.*, 2001). After the phase matching wavelength 1.31 μm the inner core fundamental mode totally relocates to outer core and vice versa. Even though the analysis is carried out for many phase matching wavelength, for discussion purpose 1.31 μm is taken into account.

Figure 3 shows the effective area of the confined inner core mode as a function of wavelength. Its noteworthy to find inner core-mode has an effective area of 1.68 μm^2 at the wavelength of 1.28 μm increases suddenly to 29.34 μm^2 after the phase matching wavelength of 1.31 μm. Similarly for the outer core mode it decreases from 29.79 to 1.7 μm^2 after the matching conditions (Sivabalan and Raina, 2011).

The dispersion of the PQF can be expressed as the sum of material dispersion and waveguide dispersion approximately. The material dispersion is also taken into consideration, since the core radius is doped with germanium. As the effective refractive index (n_{eff}) is estimated as a function of wavelength, then dispersion parameter can be computed from the Eq. (6), as:

$$D(\lambda) = -\left(\frac{\lambda}{c}\right)\left(\frac{d^2 n_{eff}}{d\lambda^2}\right) = -\left(\frac{2\pi c}{\lambda^2}\right)\left(\frac{d^2\beta}{d\omega^2}\right) \quad (6)$$

The dispersion value becomes maximum if the wavelength matches the phase matching wavelength (Subbaraman *et al.*, 2007; Zhihua *et al.*, 2008):

$$D_{max} = \pm\left(\frac{\pi}{2c\kappa}\right)\left(\frac{dn_1}{d\lambda} - \frac{dn_2}{d\lambda}\right)^2 \quad (7)$$

$$\Delta\lambda = 0.766X\left(\frac{2\kappa\lambda_p}{\pi}\right)\left|\left(\frac{dn_1}{d\lambda} - \frac{dn_2}{d\lambda}\right)^{-2}\right| \quad (8)$$

We can infer from the above equations the peak dispersion totally depends on the coupling coefficient κ and the index slope between the inner core mode and the cladding mode at phase matching wavelength (λ_p) (Zhao-yuan *et al.*, 2009). From the Eq. (7) and (8) it's evident that, if the inner-core mode and the outer-core mode are easy to couple, a big coupling constant κ is obtained, leading to a low peak dispersion value and a broad FWHM. Instead, if there is a hard coupling between the two modes, κ is small, leading to a high peak dispersion value and a narrow FWHM (Habib *et al.*, 2014; Subbaraman *et al.*, 2007). The dispersion value near the phase matching condition $\lambda_p = 1.31$ μm is observed to be -15,935 ps/(nm.km).

RESULTS

One can examine that the phase-matching wavelength shifts as a function of doping percentage, further the radius of first cladding ring is varied showing a very high deviation in the dispersion parameter. From the Fig. 4 it is evident that when $d_1 = 2.0$ μm, $d_2 = 2.0$ μm and $d_3 = 0.7$ μm, the phase matching wavelength is at 1.44 μm for an index difference of 1.92%. When index difference is increased, the phase matching value relocates towards higher wavelength of 1.451 and 1.479 μm, respectively for 1.95 and 1.98%. The dispersion value for the above index variation falls at -7,514, -7,617 and -6,835 ps/(nm-km), respectively. Eventually, when $d_1 = 2.2$ μm $d_2 = 2.0$ μm and $d_3 = 0.7$ μm the dispersion parameter takes high values of -15,881, -17,241 and -16,291 ps/(nm-km), respectively but the phase matching

wavelength decreasing to 1.309, 1.319 and 1.33 μm, respectively (Ni *et al.*, 2004).

An interesting behavior is that the dispersion parameters get shifted even when the diameter of d_2 and d_3 is altered (Han *et al.*, 2014). In Fig. 5 maintaining the values of $d_1 = 2.2$ μm, $d_2 = 2.0$ μm and d_3 was increased from 0.7 μm to 0.8 μm, the phase-matching wavelength was increased from 1.31 μm to be centred around 1.345 μm with dispersion rising to -18,164 ps/(nm-km). Likewise, when d_2 was decreased to 1.8 μm with $d_1 = 2.2$ μm and $d_3 = 0.7$ μm, the phase matching wavelength decreased to 1.28 μm with an increase in chromatic dispersion around -20,985 ps/(nm-km). We investigated various combination of diameter for the d_2 and d_3 fixing d_1 at 2.2 μm and doping with an index difference of 1.92%. In the present proposed PQF design, the number of holes with diameter d_3, d_2 and d_1 were 70, 50 and 5, respectively. The dispersion properties and phase matching wavelength of the PQF varies as a function of air filling fraction, contributed by different composition of air holes diameter. The dispersion was found to be maximum at 1.325 μm with -22,137 ps/(nm-km), for $d_2 = 1.9$ μm and $d_3 = 0.8$ μm. It was noteworthy to find that, the bandwidth is narrow when dispersion parameter was at its highest value and increased as the dispersion decreased (Mejbaul Haque *et al.*, 2014). There is generally a trade-off between the highest dispersion with bandwidth, which can be optimized by careful selection of holes diameter (Tee *et al.*, 2013).

The proposed structure of the DCF is challenging and fabrication using stack and draw method is not feasible. Complex structured PCFs with random varying holes can be fabricated by preform molded with sol-gel method (De Hazan *et al.*, 2002) and preform
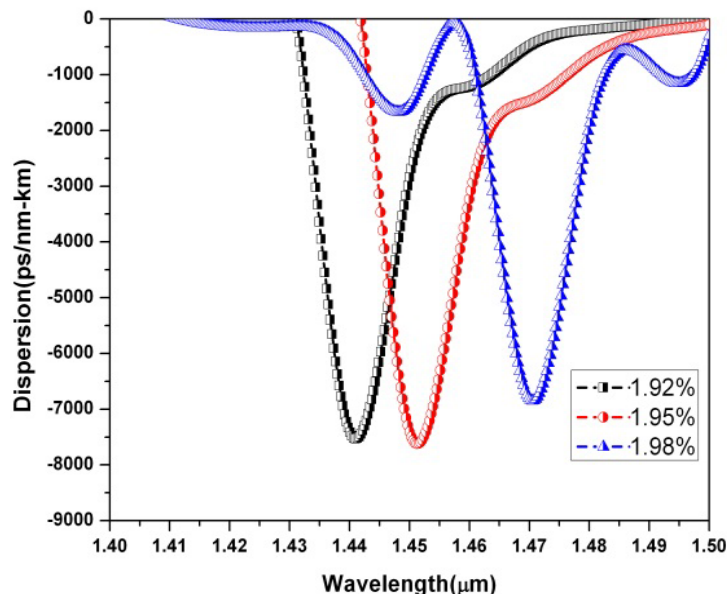
(a)
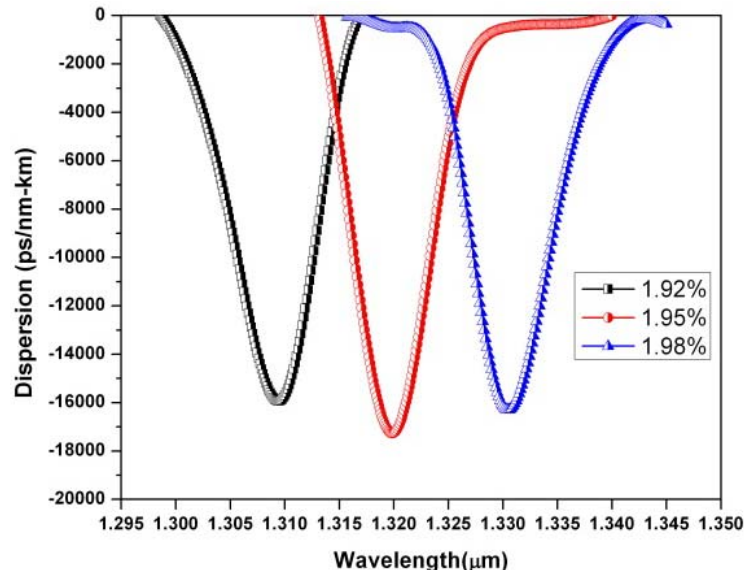
(b)

Fig. 4: Doping analysis with index difference of 1.92, 1.95 and 1.98%, respectively (a) with $d_1 = 2.0$ µm, $d_2 = 2.0$ µm, $d_3 = 0.7$ µm, (b) with $d_1 = 2.2$ µm, $d_2 = 2.0$ µm, $d_3 = 0.7$ µm
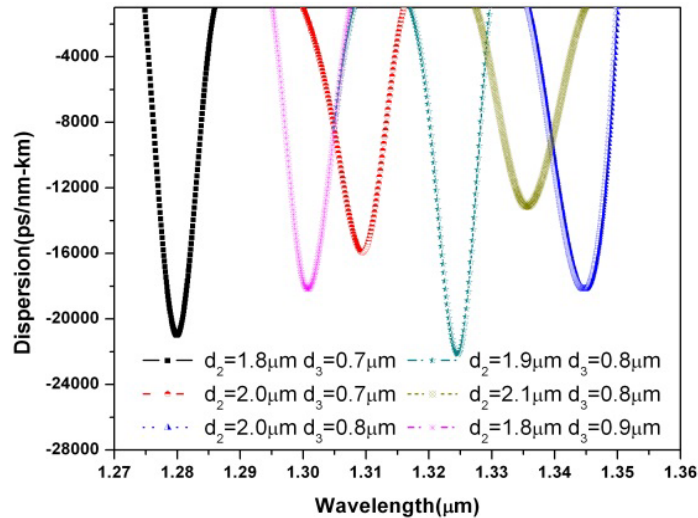

Fig. 5: Dispersion curves for a DC-PQF with fixed $d_1 = 2.2$ µm and d_2 and d_3 are variant over range of diameters with different λ_p

drilled with pattern (El-Amraoui *et al.*, 2010) with large cross-section is drawn to optimal size is a feasible technique in fabricating the complex PCF and PQF structures.

CONCLUSION

We have investigated dispersion characteristics of a novel 5-fold symmetric dual-core photonic quasi-crystal fiber. By varying the sizes of air holes, we obtained a maximum negative dispersion of -22,137 ps/(nm-km) for our proposed PQF. We also demonstrate the wide range of phase-matched wavelength (O-Band) with appropriate doping levels the range can be extended to other bands. We conclude, with optimized structural parameters and with low confinement loss, our proposed fiber is envisaged as a dispersion compensating fiber.

REFERENCES

Abdur Razzak, S.M., M.A. Rashid, Y. Namihira and A. Sayeem, 2010. Group velocity dispersion management of microstructure optical fibers. Int. J. Electr. Comput. Eng., 5(5): 298-302.

Aliramezani, M. and S. Mohammad Nejad, 2010. Numerical analysis and optimization of a dual-concentric-core photonic crystal fiber for broadband dispersion compensation. Opt. Laser Technol., 42: 1209-1217.

Birks, T.A., D. Mogilevtsev, J.C. Knight and P.S.J. Russell, 1999. Dispersion compensation using single material fibers. IEEE Photonic. Tech. L., 11: 674.

Chin-Ping, Y., L. Jia-Hong, H. Sheng-Shuo and C. Hung-Chun, 2008. Dual-core liquid-filled photonic crystal fibers for dispersion compensation. Opt. Express, 16(7): 4443.

De Hazan, Y., J.B. MacChesney, T.E. Stocker, D.J. Trevor and R.S. Windeler, 2002. Sol gel method of making an optical fiber with multiple apetures. U.S. Patent, 6,467,312 B1.

El-Amraoui, M., G. Gadret, J.C. Jules, J. Fatome, C. Fortier, F. Désévédavy, I. Skripatchev, Y. Messaddeq, J. Troles, L. Brilland, W. Gao, T. Suzuki, Y. Ohishi and F. Smektala, 2010. Microstructured chalcogenide optical fibers from As2S3 glass: Towards new IR broadband sources. Opt. Express, 18: 26655-26665.

Fleming, J.W., 1984. Dispersion in GeO2-SiO2 glasses. Appl. Opt., 23: 4486.

Gerome, F., J. Auguste and J. Blondy, 2004. Design of dispersion-compensating fibers based on a dual-concentric-core photonic crystal fiber. Opt. Lett., 29: 2725-2727.

Habib, M.S., R. Ahmad, M. Selim Habib and S.M.A. Razzak 2014. Maintaining single polarization and dispersion compensation with modified rectangular microstructure optical fiber. Optik Int. J. Light Electron. Opt., 125(3): 911-915.

Han, L., L. Liu, Z. Yu, H. Zhao, X. Song, J. Mu, X. Wu, J. Long and X. Liu, 2014. Dispersion compensation properties of dual-concentric core photonic crystal fibers. Chin. Opt. Lett., 12: 010603.

Jianfei, L., S. Junqiang, Q. Yi and D. Mingdi, 2013. Ultra-flattened chromatic dispersion and highly nonlinear photonic crystal fibers with ultralow confinement loss employing hybrid cladding. Opt. Fiber Technol., 19: 468-475.

Kim, S. and C.S. Kee, 2009. Complete photonic bandgaps in 12-fold symmetric quasicrystals. Opt. Express, 17: 15885.

Kim, S., C. Kee and J. Lee, 2007. Novel optical properties of six-fold symmetric photonic quasicrystal fibers. Opt. Express, 15: 13221-13226.

Kliros, G.S., J. Konstantinidis and C. Thraskias, 2007. Prediction of macrobending and splice losses for photonic crystal fibers based on the effective index method. WSEAS T. Commun., 8(5): 1314-1321.

Mejbaul Haque, M., M. Shaifur Rahman, M. Samiul Habib and S.M.A. Razzak, 2014. Design and characterization of single mode circular photonic crystal fiber for broadband dispersion compensation. Optik Int. J. Light Electron. Opt., 125: 2608-2611.

Ni, Y., Z. Lei, A. Liang, P. Jiangde and F. Chongcheng, 2004. Dual-core photonic crystal fiber for dispersion compensation. IEEE Photonic. Tech. L., 16: 15-16.

Sivabalan, S. and J.P. Raina, 2011. High normal dispersion and large mode area photonic quasi-crystal fiber stretcher. IEEE Photonic. Tech. L., 23: 1139-1141.

Subbaraman, H., T. Ling, Y. Jiang, M. Chen, P. Cao and R. Chen, 2007. Design of a broadband highly dispersive pure silica photonic crystal fiber. Appl. Opt., 46: 3263-3268.

Tee, D.C., M.H. Abu Bakar, N. Tamchek and F.R. Mahamd Adikan, 2013. Photonic crystal fiber in photonic crystal fiber for residual dispersion compensation over $\{rm E\} + \{rm S\} + \{rm C\} + \{rm L\} + \{rm U\}$ wavelength bands. IEEE Photonic J., 5(3).

White, T., R. McPhedran, C. De Sterke, L. Botten and M. Steel, 2001. Confinement losses in microstructured optical fibers. Opt. Lett., 26: 1660-1662.

Zhao-Yuan, S., H. Lan-Tian, Z. Xing-Tao, W. Dong-Bin, L. Xiao-Dong and L. Zhao-Lun, 2009. Study on dual-concentric-core dispersion compensation photonic crystal fiber. Braz. J. Phys., 39: 519.

Zhihua, Z., S. Yifei, B. Baomin and L. Jian, 2008. Large negative dispersion in dual-core photonic crystal fibers based on optional mode coupling. IEEE Photonic Tech. L., 20(16): 1402-1404.

Zografopoulos, D.C., C. Vazquez, E.E. Kriezis and T.V. Yioultsis, 2011. Dual-core photonic crystal fibers for tunable polarization mode dispersion compensation. Opt. Express, 19: 21680-21691.

Zoorob, M.E., M.D.B. Charlton, G.J. Parker, J.J. Baumberg and M.C. Netti, 2000. Complete photonic bandgaps in 12-fold symmetric quasicrystals. Nature, 404: 740-743.